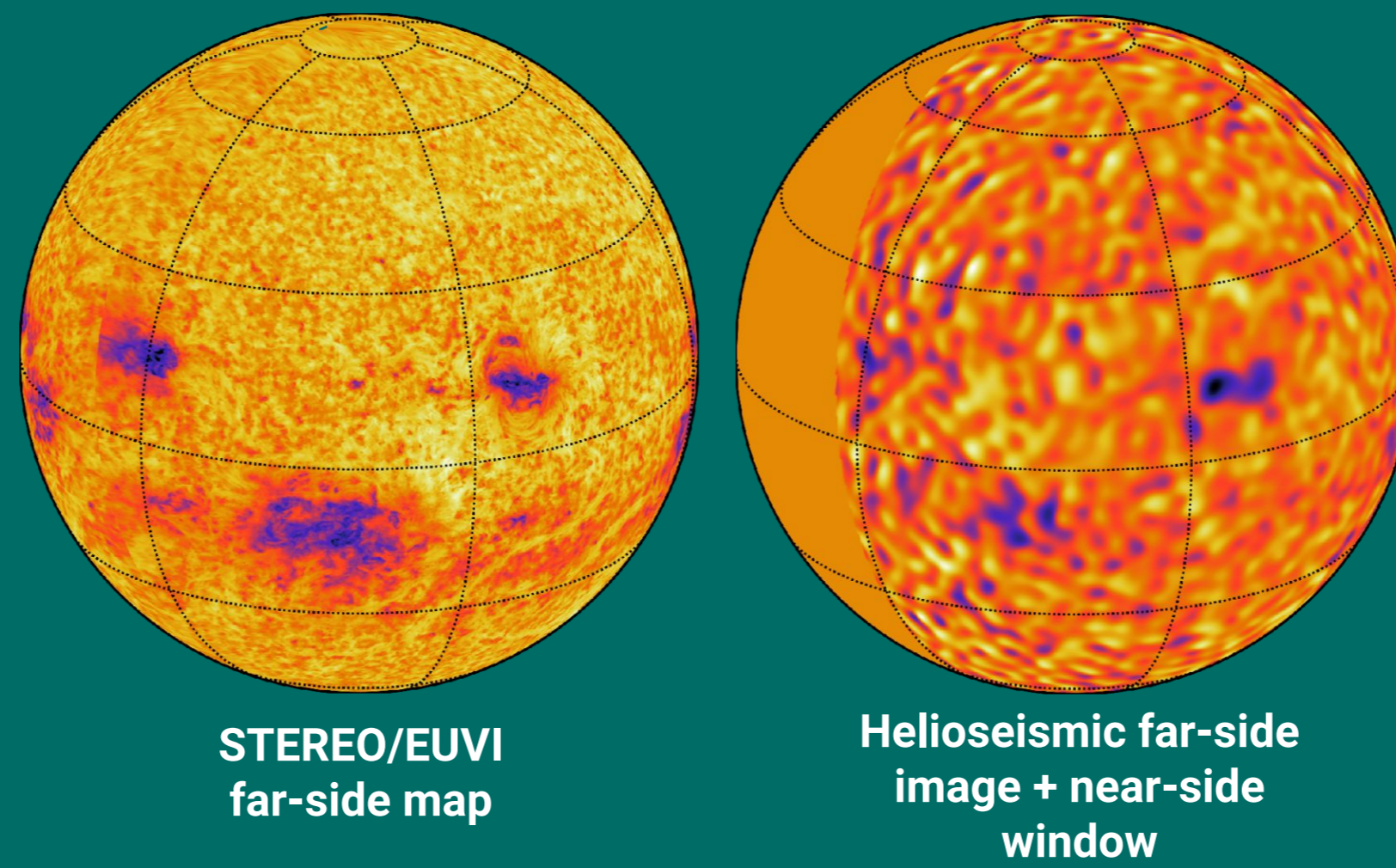


- Helioseismology can detect active regions on the Sun's far-side days before they rotate to the Earth's side, using solar acoustic oscillations.
- Recent advances in theoretical and computational helioseismology have improved far-side imaging, which enables **high-confidence detection** and daily tracking of **medium-size** active regions.



- These far-side images, however, suffer from **substantial noise**. This noise is primarily due to the stochastic nature of these solar oscillations.
- Application of **low pass filters** to the seismic phase in **spectral space** can reduce unwanted noise and quiet-Sun signatures, thereby improving the detectability of the active region signals.

Characterizing Far-Side Images in Spectral Space

1. 109-day segments from a 10-year time series of far-side images of the 24th solar cycle, mapped in the Carrington frame, were transformed into the spectral domain with a frequency resolution of 0.1 μHz . To analyze spatial characteristics, spherical harmonics were used to decompose variations into **degrees (l)** and **orders (m)**. Finally, the power spectrum was calculated.
2. A fit for lower spherical harmonic degrees ($l=0,1,2$) was removed. These degrees represent the background having high spectral leakage into high-degree modes.
3. Each segment data cube with the three parameters was averaged over 2 years of data from active and quiet periods.
4. These were then averaged over the 3 parameters to study power distribution across different scales and frequencies. This helps to get rough estimates of l , m , and ν .

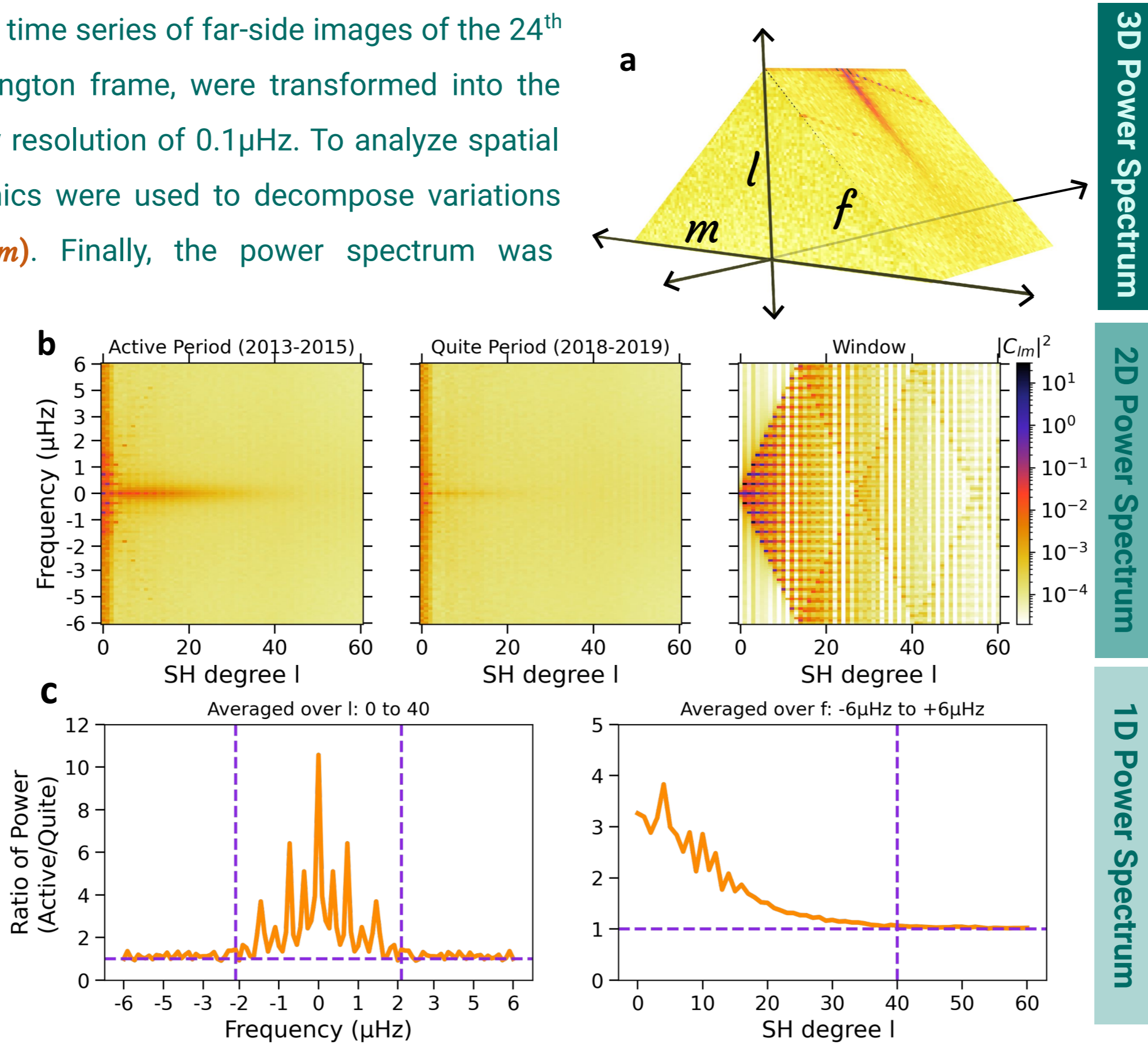


Fig 1: a) Illustrative 3D power spectrum b) 2D power spectrum averaged over all m 's for active, quiet and near-side window c) Power distribution over a signal parameter only. Indigo lines show filter limits for separating signals from noise.

Spectral filter in ν & l

A preliminary filtering process was applied in ν and l . The limits for this filtering were determined based on the analysis presented in Fig 1c i.e.

- $l > 40$
- $\nu > 2.286 \mu\text{Hz}$

in spatial and frequency domains respectively. This effectively removes surface features smaller than **100 megameters (Mm)** and temporal evolution scales faster than **5 days**.

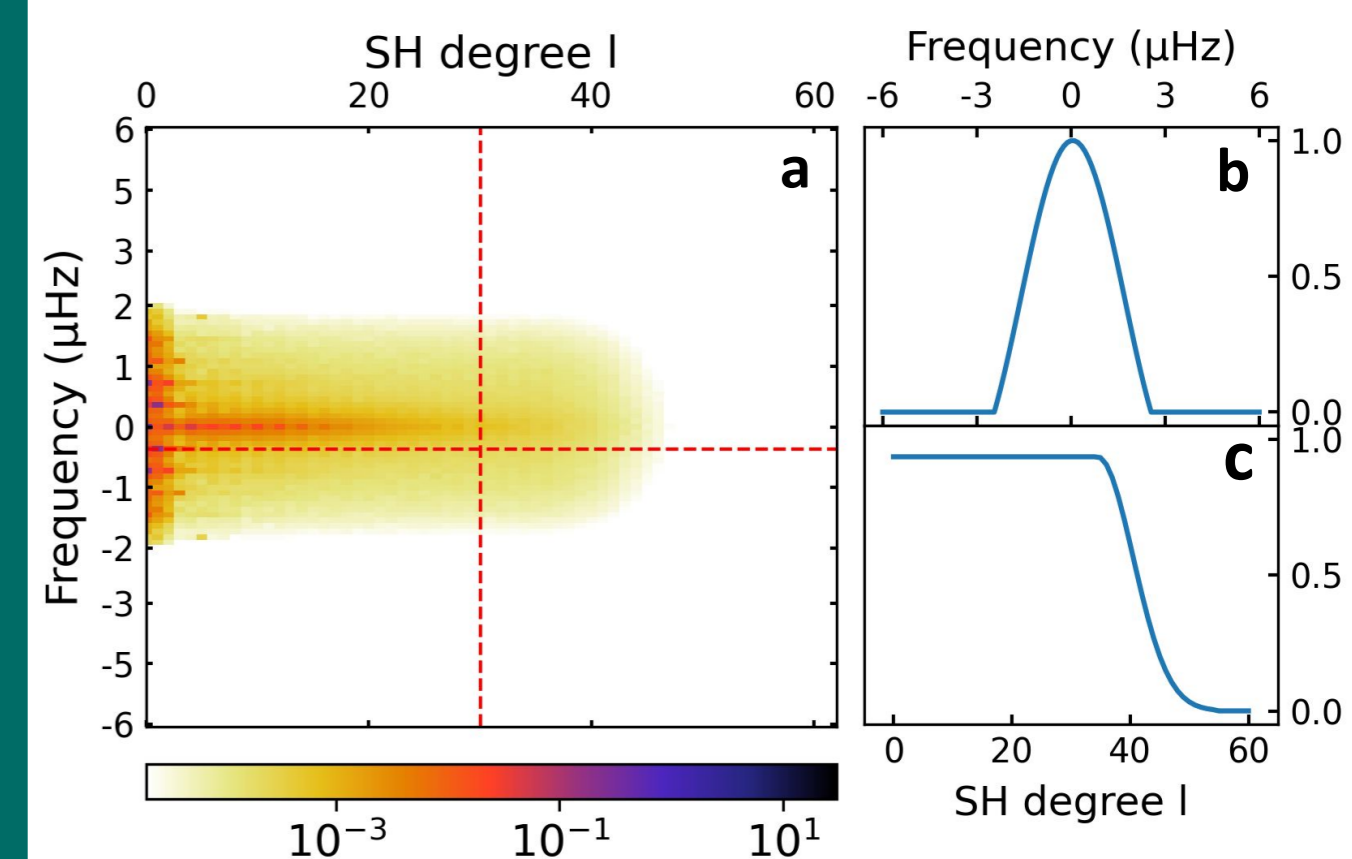


Fig 2: a) Filtered power spectrum for Fig 1d active period b) Lanczos filter in frequency ν c) Gaussian filter in spherical harmonic degree l .

Detection Statistics

The **ROC curve** is used to assess the filter's effectiveness. The diagonal line represents the performance of a random classifier. The more the curve bends from the diagonal, the better the filter performs. Even with preliminary filtering, there is an **improvement in the detection** of active regions. The true positive rate not reaching 1 may be due to an overestimation in the algorithm for detecting smaller active regions in HMI magnetograms which needs to be taken care of in the future.

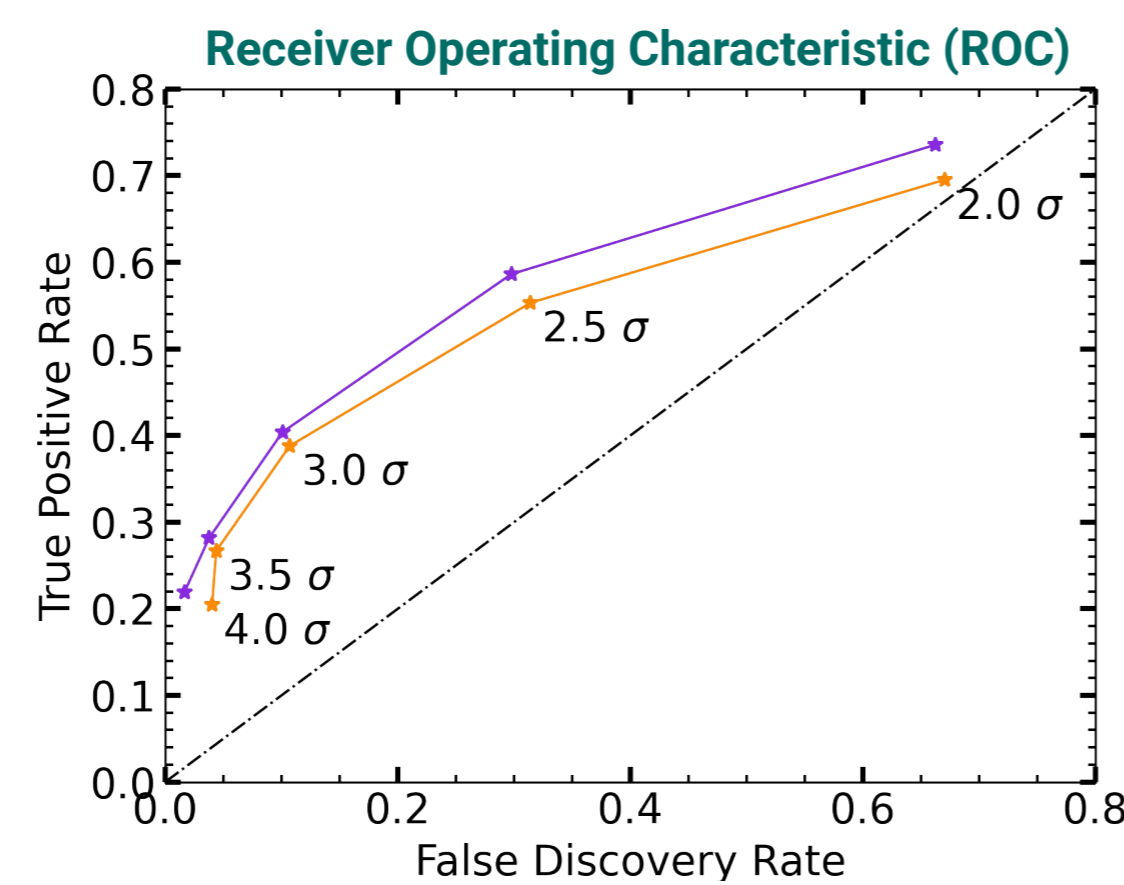


Fig 3: The ROC curves for two filters. The orange curve represents the current best filter, which utilizes a 3-day moving average in time and Gaussian smoothing in space. The indigo curve corresponds to the current filter.

Outlook: Directional Dependence

The third parameter, **spherical harmonic order m** , can also play a crucial role in eliminating artifacts from the data. To do this, excess power is certain m 's, if present, would be investigated. This could also give insight into the hypothesized **active longitudes** of the Sun. Therefore, by carefully selecting and applying filters based on the power distribution of m , we can effectively remove more unwanted noise.

The denoised dataset will provide over 10 years of data on active region (AR) evolution, serving as a valuable resource for their analysis.

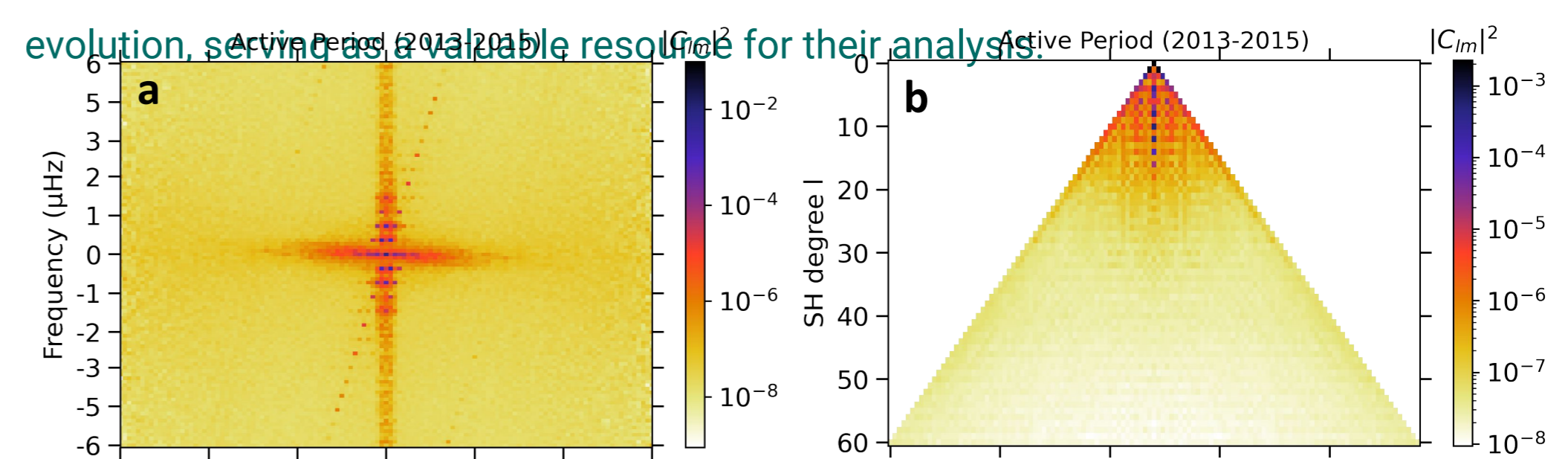


Fig 4: a) 2D power spectrum averaged over l b) 2D power spectrum averaged over ν

Affiliations

¹ Max-Planck-Institut für Sonnensystemforschung, 37077 Göttingen, Germany

² Institut für Astrophysik und Geophysik, Georg-August-Universität Göttingen, 37077 Göttingen, Germany

References

1. Gizon L, Barucq H, Duruflé M, et al. 2017, A&A, 600, A35
2. Gizon, L., Fournier, D., Yang, D., et al. 2018, A&A, 620, A136
3. Yang, D., Gizon, L., & Barucq, H. 2023, A&A, 669, A89